F and M centers in alkali halides: A theoretical study applying self-consistent dielectric-dependent hybrid density functional theory

Michael Häfner⦿ and Thomas Bredow*

Mulliken Center for Theoretical Chemistry, Institut für Physikalische und Theoretische Chemie, Universität Bonn, Beringstraße 4, 53115 Bonn, Germany

Point defects significantly change electronic properties of alkali halides and thereby enhance their reactivity. However, both the experimental and theoretical description of defects such as the F center and the M center are still far from complete, in particular for the less common bromides. A self-consistent dielectric-dependent global hybrid and plane-wave approach is employed for a comparative theoretical study of the electronic properties of NaCl, KCl, NaBr, and KBr bulk and (100) surface, both perfect and defective. For these systems, a zero-point renormalization was calculated to account for electron-phonon interaction and enhance comparability with the experiment. We focus on anion vacancy defects, the so-called F and M centers. The methodology employed is capable of reproducing measured defect level energies, electronic band gaps, ionization energies, and electron affinities within experimental errors. A general trend of the F center defect level energy with respect to the lattice parameter is found. The results for both the F and the M center of KCl agree with findings from magnetic resonance experiments. The defect orbitals are analyzed and virtual states of the defect electron are identified.

I. INTRODUCTION

The presence of defects can lead to drastic changes of the electronic structure of insulating compounds. Even unreactive substances, e.g., table salt NaCl, become reactive when point defects such as F centers are introduced. For NaCl and KCl, the reductive power of the trapped electron in surface F centers has been explored both experimentally [1–4] and theoretically [5–8]. The defect electron is transferred to adsorbed water [3,4] and salicylic acid molecules [1,2]. There exists a plethora of experimental works for the electronic structure of the pristine alkali halides. Available experimental results for pristine NaCl and KCl were summarized recently by our group [8,9]. For the bromides, there are also many experimental results for KBr [10–28] but significantly less for NaBr [12,15,16,18,20,24,27,29,30]. There are also theoretical works [9,31–40] that calculated the electronic structure of bulk and surfaces, usually employing the GW approximation. However, these studies are limited to the chlorides; no first-principles calculations of the alkali bromides were found.

F centers in alkali halides were investigated experimentally [41–54]. Most theoretical work on F centers is limited to LiF and NaCl [6,55–61], but there also exists an analysis of NaF and KCl by Zwicker [62] and an extensive analysis of the F center absorption energies for the fluorides, chlorides, and bromides of Li, Na, and K by Tiwald *et al.* [63]. Aside from Refs. [5,7,8] there are no investigations of defective surfaces available.

In recent studies of defective NaCl and KCl, we employed self-consistent dielectric-dependent global hybrid (sc-DDGH)

functionals [35,64] and were able to reproduce measured electronic properties [7,8] with an accuracy comparable to GW methods. These sc-DDGH calculations were performed with wave functions based on a linear combination of atomic orbitals (LCAO). However, a drawback of this approach is the choice of a sufficiently diffuse basis set to correctly describe the unoccupied states, because pseudolinear dependencies occur that severely affect SCF convergence and need to be addressed, in particular in slab models. In this study, we circumvented this issue by switching to a plane-wave basis.

The sc-DDGH functionals obtained with LCAO and plane waves are compared for the alkali halides NaCl, KCl, NaBr, and KBr, and it is shown that the latter provide better agreement with experimental dielectric constants. The plane-wave sc-DDGH functionals were then employed to investigate F centers in the bulk and on the (100) surface of the four alkali halides, in particular the defect level and the valence band and conduction band edge levels.

A new aspect in this study are M centers, which have been extensively investigated experimentally [65–74] and which, due to their optical properties, may serve as information carriers of optical information storage systems [75,76]. To the best of our knowledge, M centers in alkali halides, consisting of two adjacent halogen vacancies, have so far only been described once using DFT methods. Eid [77] explored the diffusion of atoms in the KBr(100) surface with M centers. We decided to study the M center in the bulk and on the (100) surface of KCl because there are experimental reference data available for this substance. We investigate the closed-shell state with two paired electrons localized in one vacancy site and two open-shell states where the defect electrons are localized in both defect sites.

---
*bredow@thch.uni-bonn.de

In the following section we provide details of our computational setup. We then compare dielectric constants obtained with LCAO and plane-wave wave functions. Plane-wave sc-DDGH is applied to defective NaCl, KCl, NaBr, and KBr.

II. COMPUTATIONAL DETAILS

We performed all calculations with the CRYSTAL17 crystalline orbital program package (version 1.0.2) [78] and the VASP 6.1.1 plane-wave program package [79–81]. For the bulk calculations with CRYSTAL we have used tight integral tolerances (7 7 7 14 42), a $8 \times 8 \times 8$ $\vec{k}$-point Monkhorst-Pack (MP) grid, and the adjusted def2-QZVPP [82] basis set from Ref. [8]. For the bulk calculations with VASP, we used the precision mode Accurate, a cutoff energy of 500 eV, and the standard pseudopotentials for the PAW method [83]. Here, the $4 \times 4 \times 4$ $\vec{k}$-point MP grid was sufficiently converged (see Supplemental Material [84]). All primitive-cell surface calculations were carried out with a $4 \times 4 \times 1$ $\vec{k}$-point MP grid, 10 layers, and 20 Å of vacuum between the repeating slabs. The defect models were calculated with a 4×4 supercell of the primitive cell for the surface and a $2 \times 2 \times 2$ supercell of the crystallographic cell for the bulk, a Γ-$\vec{k}$-point MP grid, and 20 Å vacuum distance for the surface. For the defect calculations the accuracy parameter was lowered to Normal. Both the surface F center and the M center were calculated using five-layer models. It was tested that this slab thickness is large enough to reduce defect-defect interaction to less than a tenth of an eV.

We optimized the atom positions of surface and defective models with PBE [85] and D3(BJ)-dispersion correction [86,87] using fixed lattice constants from the bulk optimizations. A structure was considered converged when all forces were <0.001 eV/Å. On average, the experimental 0 K lattice constants are overestimated by around 1%. Electronic properties were calculated using a sc-DDGH functional based on PBE that will be called sc-PBE0 in this work, following the naming convention by Fritsch *et al.* [88]. For the CRYSTAL calculations, the Fock-exchange fraction x was self-consistently calculated from the inverse of the dielectric constant ε_∞ [89–91]. With VASP, ε_∞ is calculated from the self-consistent response of the solid to a finite electric field. PBE0 with $x = 0.25$ was taken as a starting point for all self-consistent iterations of x. It has to be noted that, according to our experience, the final result for x is essentially independent from the starting point. In all cases, the Fock-exchange fraction x is used for the bulk as well as the surface models which is considered a valid strategy according to Ref. [64]. The defective surface models contain two vacancies in the top and bottom layer in order to increase symmetry and to avoid artificial dipole moments. Whenever PBE is used, the SCF calculation is carried out with the default Kosugi algorithm. For any hybrid functional calculation, a preconditioned conjugate gradient algorithm is used in the SCF procedure. Gaussian smearing is applied with a $\sigma = 0.05$ eV. Mixing of the density matrix is performed with the Kerker scheme [92] with BMIX $= 0.01$ to enhance electronic convergence. A zero-point renormalization (ZPR) of the orbital energies was calculated with PBE using the $5 \times 5 \times 5$ crystallographic

TABLE I. Comparison of the static dielectric constant ε_∞ calculated with sc-PBE0 for RT lattice parameters and experiment.

System	ε_∞			deviation (%)	
	CRYSTAL	VASP	exp.[a]	CRYSTAL	VASP
NaCl	2.262	2.308	2.329	-2.9	-0.9
KCl	2.105	2.149	2.173	-3.1	-1.1
NaBr	2.52	2.62	2.60	-3.0	0.5
KBr	2.280	2.344	2.358	-3.3	-0.6

[a]Reflectivity experiment at 290 K [98].

supercell of the bulk and a one-shot method by Zacharias and Giustino [93,94] as implemented in VASP. Convergence details can be found in the Supplemental Material [84]. The electron-phonon interaction is evaluated statistically with a Monte-Carlo sampling.

III. RESULTS AND DISCUSSION

A. Bulk properties

In the first step the Fock-exchange fraction x was self-consistently calculated as the inverse of the dielectric constant ε_∞ [35] for NaCl, KCl, NaBr, and KBr, using both room temperature (RT) and 0 K lattice parameters. The literature values of RT lattice parameters are 5.640 Å for NaCl [95], 6.288 Å for KCl [95], 5.974 Å for NaBr [96], and 6.599 Å for KBr [97]. The static dielectric constants ε_∞ obtained with VASP and CRYSTAL are compared to experimental data measured at 290 K [98] in Table I.

The plane-wave results are significantly closer (mean deviation $\sim-0.5\%$) to the experimental references than the LCAO results (mean deviation $\sim-3.0\%$). The main reason for the larger error of the LCAO results is probably the insufficient description of the polarizability of the systems with the finite-size basis. The inclusion of more diffuse functions would improve the results but leads to SCF instabilities due to pseudolinear dependencies, which are a nontrivial issue to solve. For this reason, we only used VASP for all further calculations.

In the next step we evaluated the influence of the temperature on the dielectric constant. We compared the dielectric constant calculated with the 0 K lattice constant to the measurement at 4 K [98] in Table II. The experimental lattice constants we used are 5.595 Å for NaCl [99], 6.161 Å for KCl [100], and 6.511 Å for KBr [101]. For NaBr no experimental low-temperature lattice constant was found.

TABLE II. Comparison of the static dielectric constant ε_∞ calculated with sc-PBE0 for low-temperature lattice parameters and experiment.

System	VASP	Experiment[a]	Deviation (%)
NaCl	2.330	2.351	0.9
KCl	2.211	2.204	-0.3
KBr	2.392	2.390	-0.1

[a]Reflectivity experiment at 4K [98].

TABLE III. Electronic bulk band gap E_g with RT lattice parameters.

System	NaCl (eV)	KCl (eV)	NaBr (eV)	KBr (eV)
E_g	8.80	9.07	7.13	7.70

The deviations from the experiment are smaller than 1% and the average deviation is 0.2%, well within the experimental errors. We conclude that the plane-wave sc-PBE0 method correctly describes the increase of the dielectric constant with decreasing temperature.

With the same theoretical setup we calculated the fundamental band gap E_g for all four halides. The results are given in Table III.

A comparison with experimental data is not made, since measurements that specifically measure the bulk band gap were not found for any of the halides. In contrast, alkali halides bulk band gaps were studied at various theoretical levels including GW methods [9,31–34,36–38,40,102]. Most of these first-principles studies focused on NaCl. GW methods are more sophisticated than sc-DDGH functionals and are thus expected to yield higher accuracy for electronic properties. However, due to their large computational effort, approximations have to be introduced, e.g., in the degree of self-consistency of the GW cycle or the number of bands. For these reasons, the results from the GW methods differ considerably among each other and from sc-PBE0 (see Supplemental Material [84]).

For KCl there are only two works [38,40]. The bromides were not studied using GW at all up to now.

For the surface calculations described below, we recalculated the optimal Fock exchange fraction x after optimizing the bulk lattice parameters with PBE-D3(BJ). A comparison of the optimized values of a to experimental data can be found in the Supplemental Material [84]. We obtained $x = 42.8\%$ for NaCl, $x = 46.3\%$ for KCl, $x = 37.7\%$ for NaBr, and $x = 42.4\%$ for KBr.

B. Electronic properties of the alkali halide(100) surfaces

Due to an arbitrary shift of one-electron levels in three-dimensional periodic calculations, absolute band energies are only meaningful for two-dimensional slab models. For the bulk, only the electronic band gap is physically meaningful. For the slab models, conduction band minimum (CBM) and valence band maximum (VBM) are calculated relative to the vacuum level. Convergence of the electronic properties of our models within 0.1 eV was achieved with a five-layer slab model and 20 Å of vacuum. For comparison with other theoretical studies [103], we however calculated the surfaces with ten-layer slab models. For NaBr and KBr there is no comprehensive collection of measured electronic properties in the literature, aside from a relatively small and dated analysis by Poole *et al.* [24]. As experimental references for NaCl and KCl we used our recent summaries [8,9].

To ensure a correct comparison of the experiments with the calculation, electron-phonon coupling must be considered. Unfortunately, we could not find data for any other system

than NaCl. Lambrecht *et al.* [36] calculated a ZPR of 0.167 eV for NaCl, which has to be applied to the KS-DFT band gap. We calculated the same parameter based on a one-shot Monte-Carlo sampling method [93,94] and obtained a converged ZPR correction of 0.181 eV for NaCl bulk. The deviation from the earlier result is lower than the standard deviation of the experimental measurements. The CBM and VBM energies of all halides are adjusted according to the results of the present bulk ZPR calculations. It was attempted to calculate the ZPR directly for the (100) slab models. However, the calculated ZPR did not converge with increasing surface supercell size, showing erratic behavior indicating further yet unresolved issues with the one-shot approach applied to slabs.

1. The KBr(100) surface

A considerable number of experimental studies of the electronic properties of KBr are available in the literature. In Table IV we list values obtained from an extensive literature search [10–28]. The experimental results for the electronic band gap E_g range from 7.3 to 8.05 eV with a relatively even distribution of values above and below the average value, 7.6 eV. Most of the electronic band gaps obtained more recently with modern methods such as electron energy loss spectroscopy (EELS) [27], energy distribution curves (EDC) [26], and electronic conductivity [28] are below this value. Two experiments [16,17] yield rather high band gaps of around 8 eV and may be considered as outliers. Only four values were found for the ionization potential (*IP*), ranging from 7.5 eV to 8.2 eV. Three of them lie at 8 eV or above; only Poole *et al.* found a much lower value of 7.5 eV [24]. This group generally underestimates the ionization potentials of all halides discussed in this work, therefore the corresponding values were regarded as outliers.

Most results for the electron affinity (*EA*) are obtained as the difference of *IP* and E_g. The value derived by Blechschmidt *et al.* [22] was excluded because their methodology generally overestimated *EA* for all considered systems. Only the two EDC measurements obtained *EA* directly through a data fit [25,26]. Most results for *EA* obtained as $IP - E_g$ are either about 1 eV or about 0.3 eV, while the direct results are ~0.5 eV.

The averages of the selected experimental results are 7.61 ± 0.25 eV for E_g, 7.95 ± 0.31 eV for *IP*, and 0.63 ± 0.29 eV for *EA* (Table IV). After applying a ZPR correction of 0.10 eV (0.08 eV to the VBM and 0.02 eV to the CBM) the reference values are $E_g = 7.71 \pm 0.25$, $IP = 8.03 \pm 0.31$, and $EA = 0.61 \pm 0.29$. These values are not fully consistent as the relationship $E_g = IP - EA$ is not fulfilled. This error amounts to 0.28 eV, a clear indication of a fundamental discrepancy between the various methods of determining the different electronic properties.

The sc-PBE0 results for E_g, *IP*, and *EA* of KBr(100) are 7.60 eV, 8.05 eV, and 0.45 eV, respectively. They are within the error bars of the experimental average, also after accounting for ZPR. The calculated surface band gap is 0.1 eV lower than the bulk band gap (cf. Table III). This indicates that there are no pronounced surface states in this system. It is thus expected that differences between the experimental studies are not due to the surface sensitivity of the measurement.

TABLE IV. Measured electronic properties of KBr (electronic band gap E_g, ionization potential IP, and electron affinity EA). UPS is ultraviolet-photoelectron spectrometry, EELS is electron energy loss spectroscopy, EDC is the energy distribution curve of secondary electrons emitted after irradiation with soft x rays.

Reference	Method	System	E_g (eV)	IP (eV)	EA (eV)
Mott (1985)[a]	UV absorption	Literature data			*0.7* [u]
Taft (1957)[b]	UPS	Film on LiF, 300 K		8.1	
Eby (1959)[c]	UV absorption	Film on LiF, 80 ± 2 K	7.8		*0.3*[u]
Timusk (1961)[d]	Luminescence	Single crystal, RT			*1.0*[u]
Timusk (1962)[e]	Luminescence	Single crystal, RT	7.3	8.2	*0.9*[u]
Phillips (1964)[f]	Evaluation of literature[c]	Film on LiF, 80 ± 2 K	7.8		
Metzger (1965)[g]	UPS	Films on 450Å, Al_2O_3[h]	8.05		*0.25*[u]
Huggett (1966)[i]	UV absorption/photocond.	Thin film, single crystalline, 10 K	8.0		
Fröhlich (1967)[j]	Two-photon spectroscopy	Single crystal, 20 K	7.4		
Baldini (1968)[k]	Reflectivity	Single crystal, 55 K	7.45		
Gout (1968)[l]	EELS	1000 Å films	7.6		
Blechschmidt (1970)[m]	UPS	2000–5000 Å films on Al		8.0	
Blechschmidt (1970)[n]	UPS	Thin films			*1.5–1.9*[u]
Sasaki (1971)[o]	UPS	Film on stainless steel			*0.9*[u]
Poole (1975)[p]	UPS	Single crystal		7.5	
Maruyama (1978)[q]	2nd elec. EDC (fit)	500 Å, coated with gold	7.8		0.4
Henke (1979)[r]	2nd elec. EDC (fit)	3000 Å, coated with gold	7.4		0.55
Roy (1985)[s]	EELS	Thin film on stainless steel	7.4		
Rodnyi (1989)[t]	Electronic conductivity	Literature data	7.5		
Averaged values			7.61 ± 0.25	7.95 ± 0.31	0.63 ± 0.29
ZPR corrected			7.71 ± 0.25	8.03 ± 0.31	0.61 ± 0.29
This study	sc-PBE0		7.60	8.05	0.45

[a]Reference [10].
[b]Reference [11].
[c]Reference [12].
[d]Reference [13].
[e]Reference [14].
[f]Reference [15].
[g]Reference [16].
[h]Reference [104].
[i]Reference [17].
[j]Reference [18].
[k]Reference [19].
[l]Reference [20].
[m]Reference [21].
[n]Reference [22].
[o]Reference [23].
[p]Reference [24].
[q]Reference [25].
[r]Reference [26].
[s]Reference [27].
[t]Reference [28].
[u]EA not measured directly, but calculated from the difference $IP - E_g$.

For comparison, the corresponding VASP-PBE0 ($x = 0.25$) values are $E_g = 6.31$ eV, IP $= 7.18$ eV, and EA $= 0.88$ eV. They deviate significantly from the sc-DDGH result and from experiment. This underlines the importance of self-consistent optimization of the Fock-exchange fraction x for the calculation of electronic properties.

2. The NaBr(100) surface

There are comparably few experimental data available on electronic properties of NaBr [12,15,16,18,20,24,27,29,30],

see Table V. For the ionization potential, only three values, 7.6 eV, 8.0 eV, and 7.3 eV, were found. The latter result obtained by Poole *et al.* [24] is most likely an outlier for the same reason as discussed for KBr. The electron affinity was only determined once (as $IP - E_g$); we did not find any direct measurements. Averages of the experimental results are 7.35 ± 0.30 eV for E_g and 7.63 ± 0.35 eV for IP. The reference value for EA is obtained by subtracting the averages of E_g and IP. A ZPR of 0.12 eV (0.10 eV to the VBM and 0.02 eV to the CBM) was calculated, giving experimental references 7.47 ± 0.33 eV for E_g, 7.73 ± 0.35 eV for IP, and 0.26 eV for EA.

TABLE V. Measured electronic properties of NaBr (electronic band gap E_g, ionization potential *IP*, and electron affinity *EA*) in eV. UPS is ultraviolet-photoelectron spectrometry; EELS is the electron energy loss spectrum.

Reference	Method	System	E_g (eV)	*IP* (eV)	*EA* (eV)
Eby (1959)[a]	UV absorption	Film on LiF, 80 ± 2 K	7.7		
Best (1962)[b]	EELS	Films on tungsten		7.6	
Phillips (1964)[c]	Evaluation of literature	Film on LiF, 80 ± 2 K	7.5		
Metzger (1965)[d]	UPS	Films on 450 Å Al_2O_3[j]	8.1		*0.4*[k]
Fröhlich (1967)[e]	Two-photon spectroscopy	Single crystal, 20 K	7.1		
Gout (1968)[f]	EELS	1000 Å films	7.7		
Pong (1973)[g]	UPS	Evaporated films		8.0	
Poole (1975)[h]	UPS	Single crystal		7.3	
Roy (1985)[i]	EELS	Thin film on stainless steel	7.1		
Averaged values			7.35 ± 0.30	7.63 ± 0.35	0.28[k]
ZPR corrected			7.47 ± 0.30	7.73 ± 0.35	0.26[k]
This study	sc-PBE0		7.16	8.15	0.99

[a]Reference [12].
[b]Reference [29].
[c]Reference [15].
[d]Reference [16].
[e]Reference [18].
[f]Reference [20].
[g]Reference [30].
[h]Reference [24].
[i]Reference [27].
[j]Reference [104].
[k]*EA* not measured directly but calculated from the difference $IP - E_g$.

The sc-PBE0 values for E_g, *IP*, and *EA* of NaBr(100) are 7.16 eV, 8.15 eV, and 0.99 eV, respectively. As observed for KBr(100), the surface band gap is almost the same as for the bulk (cf. Table III). For comparison, PBE0 yields E_g = 6.18 eV, IP = 7.53 eV, and EA = 1.35 eV. Similar differences between the standard and the self-consistent hybrid method are observed as for KBr.

The band gap resulting from sc-PBE0 is still within the error of the experimental reference. However, there is a clear discrepancy between our result and the average of the *IP* and several of the experimental measurements. The functional overestimates the average experimental *IP* by about 0.5 eV. The comparison is, however, difficult due to the small number of measurements and their large scatter. According to Fröhlich and Bernd [18], the electronic properties of NaBr are

more difficult to measure than for other alkali halides, and a clear determination from single-photon absorption (as, e.g., in UPS) is not easily possible. They circumvented this by using two-electron spectroscopy and obtained a band gap of 7.1 eV which is close to the theoretical result. Unfortunately, they did not measure the *IP* in that study. Considering the performance of sc-PBE0 with the other systems and the good agreement of the dielectric constant with experiment, we suggest to use the sc-PBE0 result and not the experimental average as reference for further theoretical works. Similar considerations hold for the *EA*.

3. The NaCl and KCl(100) surfaces

The electronic properties calculated with sc-PBE0 for the NaCl(100) surface are E_g = 8.60 eV, IP = 8.99 eV, and

TABLE VI. Electronic properties of NaCl and KCl(100) surfaces (electronic band gap E_g, ionization potential *IP*, and electron affinity *EA*). The zero-point correction for NaCl is calculated as 0.18 eV (0.14 eV to the VBM and 0.04 eV to the CBM); the zero-point correction for KCl is calculated as 0.18 eV (0.15 eV to the VBM and 0.03 eV to the CBM).

Reference	Method	E_g (eV)	*IP* (eV)	*EA* (eV)
NaCl				
Hochheim (2018)[a]	Literature review	8.88 ± 0.2	9.14	0.54
Hochheim (2018)[l]	LCAO-sc-PBE0	8.75	9.10	0.34
This study	VASP-sc-PBE0	8.60	8.99	0.39
KCl				
Häfner (2020)[b]	Literature review	8.72 ± 0.18	8.68 ± 0.30	0.39 ± 0.21
Häfner (2020)[c]	LCAO-sc-PBE0	8.81	8.93	0.12
This study	VASP-sc-PBE0	8.53	8.69	0.16

[a]Literature review [9].
[b]Literature review [8].

TABLE VII. Spin-up and spin-down band gaps E_g, E^*, and $E^\dagger$ of the alkali halide solids with F centers.

	NaCl (eV)	KCl (eV)	NaBr (eV)	KBr (eV)
spin-up				
E_g	9.23	9.34	7.55	7.98
E^*	4.02	3.70	3.22	3.11
spin-down				
E_g	9.45	9.52	7.85	8.20
$E^\dagger$	8.19	8.51	6.73	7.30

EA $= 0.39$ eV (Table VI). The surface band gap is about 0.2 eV smaller than the bulk band gap. This difference is slightly larger than for the bromides. For the KCl(100) surface we obtained $E_g = 8.53$ eV, IP $= 8.69$ eV, and EA $= 0.16$ eV. In this case, the band gap of the surface is about 0.55 eV smaller than the band gap of the bulk. KCl is the only system where such a large discrepancy was observed. For this system we expect larger effects in measurements of electronic properties depending on their surface sensitivity. However, this was not observed in the experiments described in Ref. [8]. This indicates that none of the experiments is able to clearly distinguish between bulk and surface results.

We compared the sc-PBE0 results to average experimental values obtained in Refs. [9] and [8]. For both systems, the calculated values are within the error bars of the experimental averages. There are small deviations (0.04–0.28 eV) from our previous calculations obtained with LCAO-sc-PBE0. Due to the use of plane waves, the results of the present study are closer to the basis set limit of the sc-PBE0 method.

C. The F center

1. Bulk F center

We examined the bulk F center (F_B) of all four halides using sc-PBE0. The calculations were performed in the doublet state. The resulting band gaps are given in Table VII. E^* is the energy difference between the defect level and the CBM. For the unoccupied (spin-down) defect levels, E^* is about 1 eV.

FIG. 2. Defect orbital of the KCl bulk F center. Isosurface cutoff $= 3$.

E_g is the energy difference between VBM and CBM. These parameters are also explained in Fig. 1.

It is found that E_g is generally larger than in the pristine bulk and smaller for the spin-up than for the spin-down ladder. We conclude that this shift is due to two counteracting effects. The first results from the Coulomb repulsion introduced by the defect electron leading to a destabilization of all low-lying unoccupied bands. The second results from the stabilizing exchange interaction of the defect electron with the lowest-lying unoccupied band because it shares its s-type character with the defect. This exchange interaction also lowers other defect bands containing s-type or p-type contribution in the defect center. For the lowest-lying unoccupied band, the effects decrease with increasing supercell size, i.e., lower defect concentration. On the other hand, for orbitals which are localized in the defect site, the effect remains significant also for larger supercells. The effect is observed both for PBE and for sc-PBE0 and is significantly larger for sc-PBE0.

E^* decreases from 4.02 eV to 3.11 eV in the series NaCl to KBr. The values are however not quantitatively related to the lattice parameters of the dielectric constants.

A graphical representation of the defect orbital is given in Fig. 2, exemplarily for KCl. For the other alkali halides the
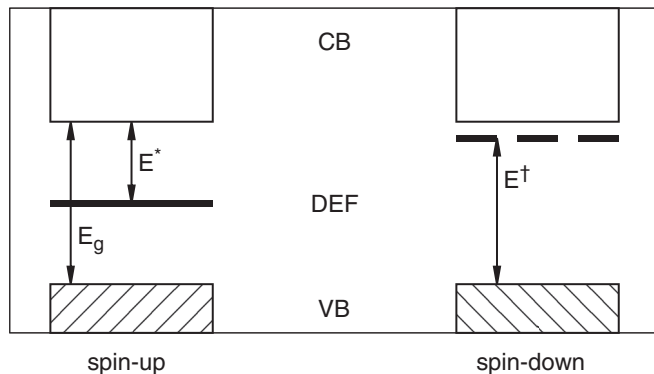

FIG. 1. Band scheme of the F center in the alkali halide bulk. The hatched bar and the solid line are occupied bands; the empty bar and the dashed line are unoccupied bands.
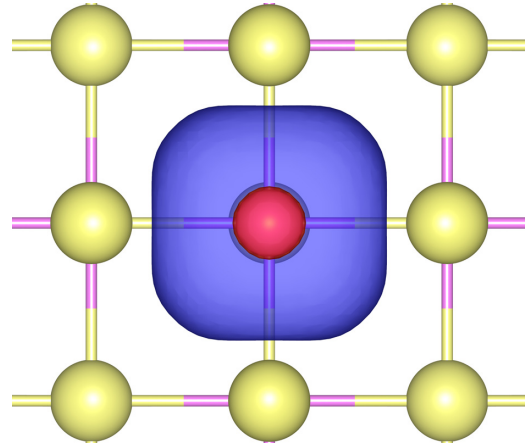
TABLE VIII. Band levels E_{def}, CBM, and VBM of the alkali halide (100) surfaces with F centers.

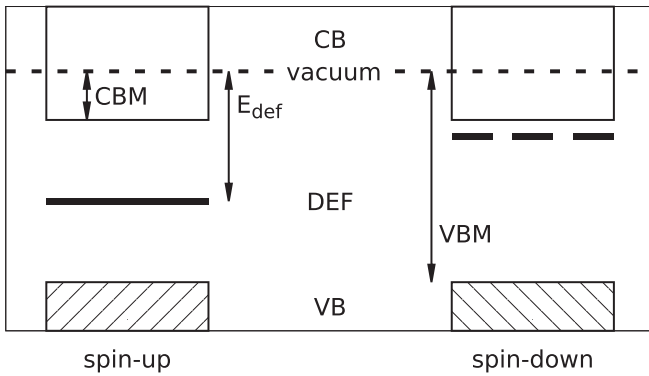|	NaCl (eV)	KCl (eV)	NaBr (eV)	KBr (eV)
spin-up				
VBM	−9.08	−8.82	−8.22	−8.12
E_{def}	−3.61	−3.12	−3.54	−3.08
CBM	−0.36	−0.19	−0.87	−0.42
spin-down				
VBM	−9.08	−8.82	−8.22	−8.12
E_{def}	−0.92	−0.48	−1.36	−0.79
CBM	−0.21	−0.05	−0.64	−0.27
pristine				
VBM	−8.99	−8.69	−8.15	−8.05
CBM	−0.39	−0.16	−0.99	−0.45

FIG. 3. Band scheme of the *F* center on the alkali halide(100) surface. The hatched bar and the solid line are occupied bands; the empty bar and the dashed line are unoccupied bands. The narrow dotted line indicates the vacuum reference.

FIG. 4. E_{def} as a function of $1/a$ for NaCl(100), KCl(100), NaBr(100), and KBr(100).

defect orbitals have similar shape. It is basically a diffuse *s*-type function but with some *p*-type contributions due to the interaction with the neighboring ions. This in line with magnetic spin resonance experiments conducted on the NaCl *F* center [105–110].

We also identified three degenerate virtual defect orbitals with a strong *p*-type contribution. They are similar to the orbitals calculated for LiF in Ref. [56]. The *p*-type orbitals are responsible for the first optical transition observed in measurements of the F_B center [52]. A depiction of those orbitals can be found in the Supplemental Material [84].

2. (100) surface F center

The electronic properties of the (100) surface *F* center (F_S) obtained with sc-PBE0 are given in Table VIII. The defective slab models are calculated as singlet or triplet states, since they contain two defects. The energies of both occupied and unoccupied defect levels relative to the vacuum level are denoted as E_{def}. The VBM are almost identical for spin-up and spin-down bands, also the CBM are similar. Here, the variation comes again from the diffuse, delocalized character of the conduction band and the interaction with the unoccupied defect level. All parameters are also explained in Fig. 3. The unoccupied spin-down defect levels are 0.43–0.72 eV below the CBM.

To the best of the authors' knowledge, no experiment has been conducted to measure these electronic properties. In a previous theoretical study Krumhansl and Schwartz [111] calculated the energy of the 1*s* defect level, which corresponds to our E_{def}. For NaCl (KCl) they obtained −3.85 (−3.18) eV, quite close to our results, −3.61 and −3.12 eV, respectively. They based their calculations on a $1/r$ Coulomb-like term for the ground state energy, where *r* is the radius of the defect cavity. We tested this hypothesis by plotting E_{def} vs $1/a$ (Fig. 4), assuming proportionality of *a* and *r*.

The correlation of data to the linear fit is reasonable ($R^2 = 0.898$). This confirms that the absolute defect level generally adheres to this relationship. Linear extrapolation of E_{def} to $1/a \rightarrow 0$ (corresponding to a free electron) is indeed close to 0 eV.
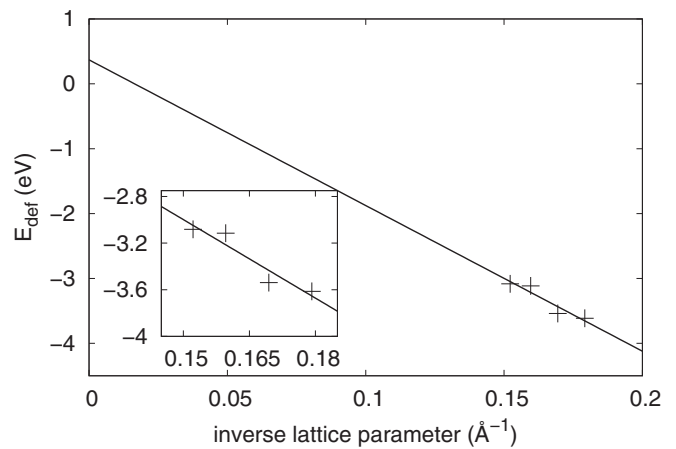
The surface defect orbital is not as symmetric as the bulk defect orbital [Fig. 5(a)]. It significantly extends into the vacuum region above the surface. Since the defect orbitals of all alkali halide surfaces have similar shape, we only show graphs for KCl(100).

Similar excited *p*-type states as observed for the bulk defect are found on the defective (100) surface. Due to site-symmetry lowering ($O_h \rightarrow C_{4v}$) the three formerly degenerate states split into a lower A_1 state [Fig. 5(b)] and two *E* states with
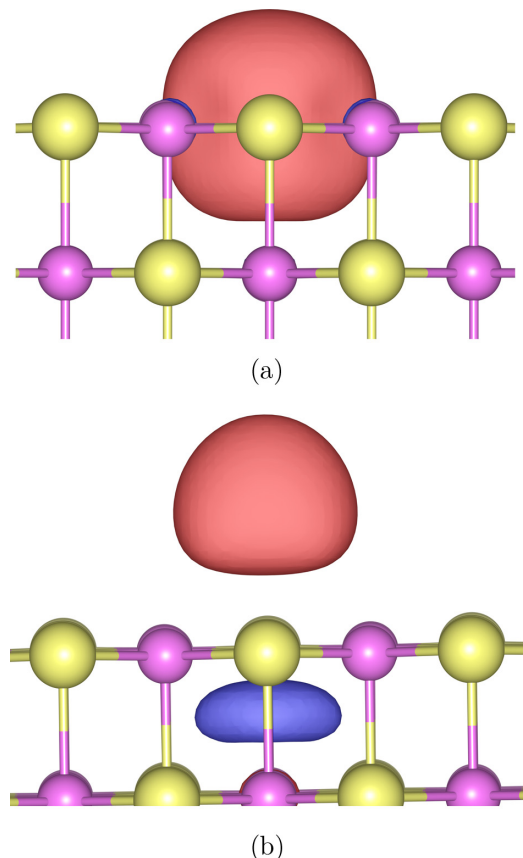

(a)

(b)

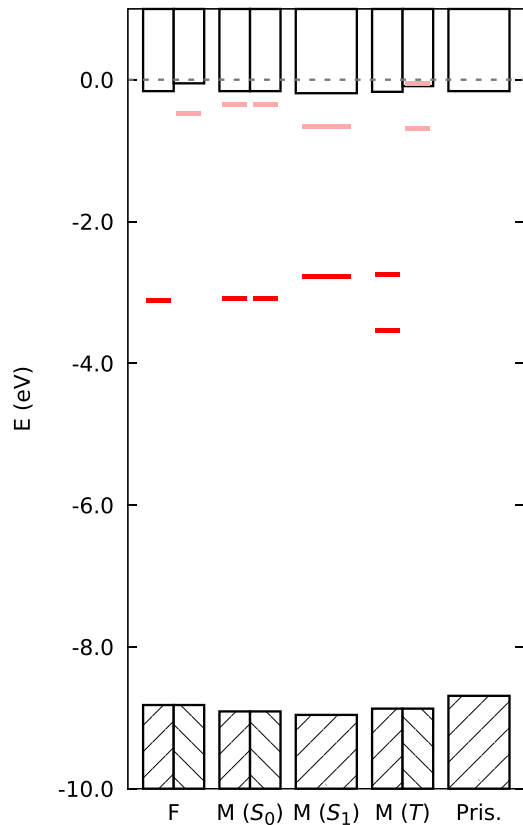FIG. 5. *F* center on the KCl(100) surface.

FIG. 6. Energy diagram of the pristine and defective KCl(100) surface. Red levels are occupied defect bands; pink levels are unoccupied defect bands.

higher energy. The lowering of the A_1 state is probably caused by a reduced Coulomb repulsion. A depiction of the E states is given in the Supplemental Material [84].

The spin-down band edges of defective and pristine surfaces do not differ significantly (Table VIII). Coupling of the valence and conduction bands with the localized spin-up defect states is small.

D. *M* centers

The M center (initially denoted as R_2 center by Seitz [52]) consists of two adjacent F centers. We calculated its properties for both the KCl bulk and the KCl(100) surface. To the best of the authors' knowledge, there has not been such a theoretical investigation of this defect type in the alkali halides yet.

The two defect electrons may be localized in separate defect sites in a triplet (T) or open-shell singlet state (S_0) or occupy the same defect orbital in a closed-shell singlet state (S_1). At sc-PBE0 level the open-shell singlet state is the ground state. The open-shell singlet is 0.24 eV lower than the closed-shell singlet and 0.78 eV lower than the triplet state. Previous experiments [70–74] concluded that the M center is not paramagnetic, which is consistent with our results. A distinction between S_0 or S_1 was not made in the experiments.

The electronic properties of all M center states, the F center, and the pristine (100) surface of KCl are shown in
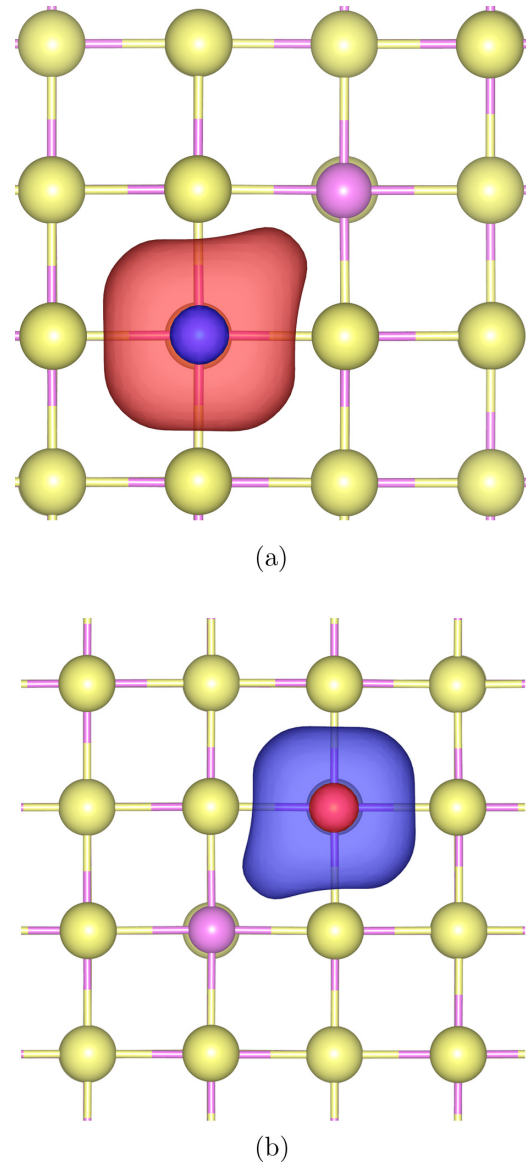

FIG. 7. *M* center in KCl bulk (S_0).

Fig. 6. Detailed results for the different M center states can be found in the Supplemental Material [84].

The occupied defect orbitals of the S_0 state are shown in Fig. 7. They have almost identical shapes but are confined in neighboring defect sites.

Compton and Rabin concluded that the M center is responsible for the so-called M band [65] which is the most prominent defect band aside from the F band. The S_0 state of the M center has two low-lying unoccupied defect orbitals (at -0.37 eV, shown in Fig. 6). They are located in the respective other cavity compared to their occupied counterparts. The M center excitation from the occupied to the unoccupied defect state is lower than the F center $1s \rightarrow 2p$ excitation, which is in agreement with the experimental observation by Petroff [69]. Okamoto [70] as well as Rolfe and Morrison [67] further analyzed the M band and found a second band overlapping with the F band. This was interpreted by Rolfe and Morrison [67] as transition from the occupied M center orbitals to

2*p*-type orbitals (shown in the Supplemental Material [84]). Our results are in good agreement with this explanation. Due to symmetry lowering and electron-electron interaction, the 2*p*-type states are split compared to the *F* center 2*p*-type state.

The occupied defect level energies of *F* and *M* centers (S_0 state) are quite similar, -3.05 eV compared to $-3.09/-3.08$ eV. This indicates that the coupling between the electrons in the *M* center is small. Reduction of adsorbed molecules should be quite similar on both defect types. However, a two-electron reduction may take place on the *M* center.

As a concluding remark, Zahrt *et al.* [66] measured the thermodynamic properties of the *M* center in KCl and determined that the enthalpy of the *M* center formation from two separate *F* centers is -0.18 eV$/M$ center. With sc-PBE0 we obtained an energy difference of -0.29 eV$/M$ center which is quite similar.

IV. CONCLUSIONS

The electronic properties of the four alkali halides NaCl, KCl, NaBr, and KBr were calculated using a self-consistent hybrid functional based on the PBE exchange-correlation functional. Using a plane-wave approach we were able to reproduce experimental measurements for both the solid and the surface within the experimental error range. The zero-point renormalization was calculated for all systems. The *F* centers in the bulk and on the (100) surface of all four halides were investigated with sc-PBE0. For the bulk, the defect levels are 4–5 eV above the VBM and 3–4 eV below the CBM. There is no quantitative correlation between the defect level position and the lattice parameters or the dielectric constants. Therefore local interactions with neighboring ions must be responsible for the observed changes. On the other hand, the binding energy of the surface defect level is in good approximation proportional to the inverse lattice constant. Both bulk and surface defect orbitals are highly localized at the vacancy sites. The interaction of the defect electrons with the delocalized electrons in the valence and conduction bands is small. The shape of the occupied (1*s*-type) and unoccupied (2*p*-type) defect orbitals is in line with experimental measurements and other theoretical investigations. The *M* center was investigated at DFT level. The results for the nature of the ground state are in agreement with experimental observations. It was also possible to identify the defect orbitals associated with the different *M* center excitations.

[1] C. Tegenkamp and H. Pfnür, Phys. Chem. Chem. Phys. **4**, 2653 (2002).

[2] U. Malaske, C. Tegenkamp, M. Henzler, and H. Pfnür, Surf. Sci. **408**, 237 (1998).

[3] S. Fölsch and M. Henzler, Surf. Sci. **247**, 269 (1991).

[4] U. Malaske, H. Pfnür, M. Bässler, M. Weiss, and E. Umbach, Phys. Rev. B **53**, 13115 (1996).

[5] W. Chen, C. Tegenkamp, H. Pfnür, and T. Bredow, Phys. Rev. B **79**, 235419 (2009).

[6] W. Chen, C. Tegenkamp, H. Pfnür, and T. Bredow, Phys. Rev. B **82**, 104106 (2010).

[7] M. Hochheim and T. Bredow, J. Phys. Chem. C **122**, 29426 (2018).

[8] M. Häfner, M. Hochheim, and T. Bredow, J. Phys. Chem. C **124**, 12606 (2020).

[9] M. Hochheim and T. Bredow, Phys. Rev. B **97**, 235447 (2018).

[10] N. F. Mott, Trans. Faraday Soc. **34**, 500 (1938).

[11] E. Taft and H. Philipp, J. Phys. Chem. Solids **3**, 1 (1957).

[12] J. E. Eby, K. J. Teegarden, and D. B. Dutton, Phys. Rev. **116**, 1099 (1959).

[13] T. Timusk, J. Phys. Chem. Solids **18**, 265 (1961).

[14] T. Timusk and W. Martienssen, Phys. Rev. **128**, 1656 (1962).

[15] J. C. Phillips, Phys. Rev. **136**, A1705 (1964).

[16] P. H. Metzger, J. Phys. Chem. Solids **26**, 1879 (1965).

[17] G. R. Huggett and K. Teegarden, Phys. Rev. **141**, 797 (1966).

[18] D. Fröhlich and B. Staginnus, Phys. Rev. Lett. **19**, 496 (1967).

[19] G. Baldini and B. Bosacchi, Phys. Rev. **166**, 863 (1968).

[20] C. Gout and F. Pradal, J. Phys. Chem. Solids **29**, 581 (1968).

[21] D. Blechschmidt, M. Skibowski, and W. Steinmann, Phys. Status Solidi B **42**, 61 (1970).

[22] D. Blechschmidt, M. Skibowski, and W. Steinmann, Opt. Commun. **1**, 275 (1970).

[23] T. Sasaki, Y. Iguchi, H. Sugawara, S. Sato, T. Nasu, A. Fjiri, S. Onari, K. Kojima, and T. Oya, J. Phys. Soc. Jpn. **30**, 580 (1971).

[24] R. T. Poole, J. G. Jenkin, J. Liesegang, and R. C. G. Leckey, Phys. Rev. B **11**, 5179 (1975).

[25] I. Maruyama and R. Onaka, J. Phys. Soc. Jpn. **44**, 196 (1978).

[26] B. L. Henke, J. Liesegang, and S. D. Smith, Phys. Rev. B **19**, 3004 (1979).

[27] G. Roy, G. Singh, and T. Gallon, Surf. Sci. **152–153**, 1042 (1985).

[28] P. A. Rodnyi, Sov. Phys. J. **32**, 476 (1989).

[29] P. E. Best, Proc. Phys. Soc. **79**, 133 (1962).

[30] W. Pong and J. A. Smith, Phys. Rev. B **7**, 5410 (1973).

[31] S. Botti and M. A. L. Marques, Phys. Rev. Lett. **110**, 226404 (2013).

[32] W. Chen and A. Pasquarello, Phys. Rev. B **86**, 035134 (2012).

[33] I.-H. Chu, J. P. Trinastic, Y.-P. Wang, A. G. Eguiluz, A. Kozhevnikov, T. C. Schulthess, and H.-P. Cheng, Phys. Rev. B **93**, 125210 (2016).

[34] A. L. Kutepov, Phys. Rev. B **95**, 195120 (2017).

[35] J. H. Skone, M. Govoni, and G. Galli, Phys. Rev. B **89**, 195112 (2014).

[36] W. R. L. Lambrecht, C. Bhandari, and M. van Schilfgaarde, Phys. Rev. Mater. **1**, 043802 (2017).

[37] E. L. Shirley, Phys. Rev. B **58**, 9579 (1998).

[38] M. J. van Setten, M. Giantomassi, X. Gonze, G.-M. Rignanese, and G. Hautier, Phys. Rev. B **96**, 155207 (2017).

[39] A. Dittmer, R. Izsák, F. Neese, and D. Maganas, Inorg. Chem. **58**, 9303 (2019).

[40] L. Hedin, Jo. Phys. Condens. Matter **11**, R489 (1999).

[41] H. Rabin and C. C. Klick, Phys. Rev. **117**, 1005 (1960).

[42] J. M. Worlock and S. P. S. Porto, Phys. Rev. Lett. **15**, 697 (1965).

[43] G. Benedek and G. F. Nardelli, Phys. Rev. **154**, 872 (1967).

[44] C. J. Buchenauer and D. B. Fitchen, Phys. Rev. **167**, 846 (1968).

[45] L. F. Stiles, M. P. Fontana, and D. B. Fitchen, Phys. Rev. B **2**, 2077 (1970).

[46] M. Ghomi, E. Rzepka, and L. Taurel, Phys. Status Solidi B **92**, 447 (1979).

[47] M. Ghomi and J. P. Buisson, J. Phys. Condens. Matter **12**, 4631 (1979).

[48] R. T. Williams, B. B. Craig, and W. L. Faust, Phys. Rev. Lett. **52**, 1709 (1984).

[49] J. Dickinson, S. Orlando, S. Avanesyan, and S. Langford, Appl. Phys. A **79**, 859 (2004).

[50] T. Koyama, M. Nakajima, and T. Suemoto, J. Phys. Soc. Jpn. **78**, 075002 (2009).

[51] A. Perregaux and G. Ascarelli, Phys. Rev. B **10**, 1683 (1974).

[52] F. Seitz, Rev. Mod. Phys. **26**, 7 (1954).

[53] U. M. Grassano, G. Margaritondo, and R. Rosei, Phys. Rev. B **2**, 3319 (1970).

[54] L. D. Bogan and D. B. Fitchen, Phys. Rev. B **1**, 4122 (1970).

[55] M. R. Pederson and B. M. Klein, Phys. Rev. B **37**, 10319 (1988).

[56] F. Karsai, P. Tiwald, R. Laskowski, F. Tran, D. Koller, S. Gräfe, J. Burgdörfer, L. Wirtz, and P. Blaha, Phys. Rev. B **89**, 125429 (2014).

[57] G. Mallia, R. Orlando, C. Roetti, P. Ugliengo, and R. Dovesi, Phys. Rev. B **63**, 235102 (2001).

[58] J.-i. Adachi and N. Kosugi, Bull. Chem. Soc. Jpn. **66**, 3314 (1993).

[59] C. M. Fang and R. A. de Groot, J. Phys. Condens. Matter **20**, 075219 (2008).

[60] H. A. Kassim and M. M. Uoda, J. Univ. Babylon Pure Appl. Sci. **26**, 173 (2018).

[61] A. Popov, E. Kotomin, and J. Maier, Nucl. Instrum. Methods Phys. Res. B **268**, 3084 (2010).

[62] R. D. Zwicker, Phys. Rev. B **18**, 2004 (1978).

[63] P. Tiwald, F. Karsai, R. Laskowski, S. Gräfe, P. Blaha, J. Burgdörfer, and L. Wirtz, Phys. Rev. B **92**, 144107 (2015).

[64] J. H. Skone, M. Govoni, and G. Galli, Phys. Rev. B **93**, 235106 (2016).

[65] W. D. Compton and H. Rabin, *F-Aggregate Centers in Alkali Halide Crystals*, edited by F. Seitz and D. Turnbull, Solid State Physics, Vol. 16 (Academic, New York, 1964), pp. 121–226.

[66] J. D. Zahrt, A. B. Scott, and E. H. Coker, J. Chem. Phys. **46**, 791 (1967).

[67] J. Rolfe and S. R. Morrison, Phys. Rev. B **15**, 3211 (1977).

[68] E. R. Hodgson, A. Delgado, and J. L. A. Rivas, J. Phys. Condens. Matter **12**, 1239 (1979).

[69] S. Petroff, Z. Phys. **127**, 443 (1950).

[70] F. Okamoto, Phys. Rev. **124**, 1090 (1961).

[71] P. R. Moran, S. H. Christensen, and R. H. Silsbee, Phys. Rev. **124**, 442 (1961).

[72] H. Ohkura and K. Murase, J. Phys. Soc. Japan **16**, 2076 (1961).

[73] E. Sonder, Phys. Rev. **125**, 1203 (1962).

[74] H. Seidel and H. C. Wolf, Phys. Status Solidi B **11**, 3 (1965).

[75] T. J. Turner, R. De Batist, and Y. Haven, Phys. Status Solidi B **11**, 535 (1965).

[76] I. Schneider, M. Marrone, and M. N. Kabler, Appl. Opt. **9**, 1163 (1970).

[77] K. M. Eid, Egypt. J. Sol. **23**, 189 (2000).

[78] R. Dovesi, A. Erba, R. Orlando, C. M. Zicovich-Wilson, B. Civalleri, L. Maschio, M. Rérat, S. Casassa, J. Baima, S. Salustro, and B. Kirtman, Wiley Interdiscip. Rev.: Comput. Mol. Sci. **8**, e1360 (2018).

[79] G. Kresse and J. Hafner, Phys. Rev. B **47**, 558 (1993).

[80] G. Kresse and J. Furthmüller, Comput. Mater. Sci. **6**, 15 (1996).

[81] G. Kresse and J. Furthmüller, Phys. Rev. B **54**, 11169 (1996).

[82] F. Weigend, F. Furche, and R. Ahlrichs, J. Chem. Phys. **119**, 12753 (2003).

[83] G. Kresse and D. Joubert, Phys. Rev. B **59**, 1758 (1999).

[84] See supplemental material at http://link.aps.org/supplemental/10.1103/PhysRevB.102.184108 for convergence tests and further orbital depictions.

[85] J. P. Perdew, K. Burke, and M. Ernzerhof, Phys. Rev. Lett. **77**, 3865 (1996).

[86] S. Grimme, S. Ehrlich, and L. Goerigk, J. Comput. Chem. **32**, 1456 (2011).

[87] S. Grimme, J. Antony, S. Ehrlich, and H. Krieg, J. Chem. Phys. **132**, 154104 (2010).

[88] D. Fritsch, B. J. Morgan, and A. Walsh, Nanoscale Res. Lett. **12**, 19 (2017).

[89] M. Ferrero, M. Rérat, B. Kirtman, and R. Dovesi, J. Chem. Phys. **129**, 244110 (2008).

[90] M. Ferrero, M. Rérat, R. Orlando, and R. Dovesi, J. Comput. Chem. **29**, 1450 (2008).

[91] M. Ferrero, M. Rérat, R. Orlando, and R. Dovesi, J. Chem. Phys. **128**, 014110 (2008).

[92] G. P. Kerker, Phys. Rev. B **23**, 3082 (1981).

[93] M. Zacharias, C. E. Patrick, and F. Giustino, Phys. Rev. Lett. **115**, 177401 (2015).

[94] M. Zacharias and F. Giustino, Phys. Rev. B **94**, 075125 (2016).

[95] D. Walker, P. K. Verma, L. M. Cranswick, R. L. Jones, S. M. Clark, and S. Buhre, Am. Mineral. **89**, 204 (2004).

[96] V. T. Deshpande, Acta Crystallogr. **14**, 794 (1961).

[97] O. D. Slagle and H. A. McKinstry, Acta Crystallogr. **21**, 1013 (1966).

[98] R. P. Lowndes, D. H. Martin, and L. F. Bates, Proc. R. Soc. Lond. A Math. Phys. Sci. **308**, 473 (1969).

[99] V. N. Staroverov, G. E. Scuseria, J. Tao, and J. P. Perdew, Phys. Rev. B **78**, 239907(E) (2008).

[100] R. Rodriguez, M. M. Barboza-Flores, R. Perez, and A. B. Clark, Eur. J. Phys. **13**, 189 (1992).

[101] W. T. Berg, J. A. Morrison, and E. W. R. Steacie, Proc. R. Soc. Lond. A Math. Phys. Sci. **242**, 467 (1957).

[102] A. L. Kutepov, Phys. Rev. B **94**, 155101 (2016).

[103] A. Grüneis, G. Kresse, Y. Hinuma, and F. Oba, Phys. Rev. Lett. **112**, 096401 (2014).

[104] S. W. Duckett and P. H. Metzger, Phys. Rev. **137**, A953 (1965).

[105] C. Kittel and E. Abrahams, Phys. Rev. **90**, 238 (1953).

[106] C. A. Hutchinson, Phys. Rev. **75**, 1769 (1949).

[107] C. A. Hutchison and G. A. Noble, Phys. Rev. **87**, 1125 (1952).

[108] A. H. Kahn and C. Kittel, Phys. Rev. **89**, 315 (1953).

[109] A. F. Kip, C. Kittel, R. A. Levy, and A. M. Portis, Phys. Rev. **91**, 1066 (1953).

[110] A. M. Portis, Phys. Rev. **91**, 1071 (1953).

[111] J. A. Krumhansl and N. Schwartz, Phys. Rev. **89**, 1154 (1953).